Kinetic Property of Bulged Helix Formation: Analysis of Kinetic Behavior Using Nearest-Neighbor Parameters

Tatsuo Ohmichi,[†] Hiroyuki Nakamuta,[‡] Kyohko Yasuda,[†] and Naoki Sugimoto*[,†,‡]

Contribution from the High Technology Research Center, and Department of Chemistry, Faculty of Science, Konan University, 8-9-1 Okamoto, Higashinada-ku, Kobe 658-8501, Japan

Received May 22, 2000

Abstract: Bulge structure is one of the well-known and important nucleic acid secondary structures containing unpaired nucleotides. Although the thermodynamic property has been thoroughly investigated, the detailed kinetic property of the bulged helix formation is still unknown. We now investigated the helix formation mechanism for bulged helices using temperature-jump experiments. The activation energy for the duplex association (E_{a+1}) obtained from the temperature dependence of the rate constants showed that the E_{a+1} value depended on both the bulged nucleotide and its flanking base pairs. The activation energy for duplex dissociation (E_{a-1}), however, did not always depend on the bulged nucleotide. In the case of d(TAGCGTTATAA)/d(ATCCAATATT) with one C bulge (GCG-bulge helix) and d(TAGAGTTATAA)/d(ATCCAATATT) with one A bulge (GAG-bulge helix), that had different bulged nucleotides and the same flanking base-pairs, the E_{a+1} value of −13.5 kcal/mol for the GCG-bulge helix was 11.9 kcal/mol more negative than the value of −1.6 kcal/mol for the GAG-bulge helix. The E_{a-1} value of 50.9 kcal/mol for the GCG-bulge helix was, however, close to 48.7 kcal/mol of the GAG-bulge helix. These data indicate that the rate-limiting steps for both the GCG-bulge and GAG-bulge helices are likely to be the same step. Furthermore, since it was known that fully matched helix formations can be estimated using nearest-neighbor parameters [Williams, A. P.; Longfellow, C. E.; Freier, S. M.; Kierzek, R.; Turner, D. H *Biochemistry* **1989**, *28*, 4283−4291], the kinetic data for a bulged helix were also analyzed and found analogous to the fully matched double helices. As a result, we found that the energy diagrams of the helix formations for bulged helices could be estimated using nearest-neighbor parameters for the DNA/DNA helix. According to these diagrams, the rate-limiting step for bulged helices can be considered to be the formation of four or five base pairs containing one bulged nucleotide. These results showed that the analysis of the kinetic behavior using nearest-neighbor parameters is a feasible approach and makes possible the understanding and prediction of folding in the unpaired regions of nucleic acids.

Introduction

To investigate the biological roles of DNAs and RNAs, it is necessary to study the relationship between their function and structure. From the standpoint of biophysical chemistry, thermodynamic and kinetic information was obtained to provide the understanding and prediction of such a relationship from the nucleic acid sequence. From a thermodynamic standpoint, the duplex stabilities of the Watson−Crick and non-Watson−Crick pairs predicted by a nearest-neighbor model can be used to investigate antisense, ribozymes, or DNA and RNA folding studies.[1−3] This nearest-neighbor model assumes that the stability of the base pair depends on the identity of the adjacent base pairs. This model has been applied to DNA/DNA, RNA/RNA, and RNA/DNA Watson−Crick pairs and DNA/DNA and RNA/RNA non-Watson−Crick pairs.[4−8] Furthermore, the thermodynamic data for nucleoside analogues have been investigated in order to understand the stacking and hydrogen-bonding interactions.[9]

* To whom correspondence should be addressed.
[†] High Technology Research Center, Konan University.
[‡] Department of Chemistry, Faculty of Science, Konan University.

(1) (a) Hertel, K. J.; Stage-Zimmermann, T. K.; Ammons, G.; Uhlenbeck, O. C. *Biochemistry* **1998**, *37*, 16983−16988. (b) Wu, M.; Tinoco, I., Jr. *Proc. Natl. Acad. Sci. U.S.A.* **1998**, *95*, 11555−11560. (c) Stage-Zimmermann, T. K.; Uhlenbeck, O. C. *RNA* **1998**, *4*, 875−889. (d) Testa, S. M.; Gryaznov, S. M.; Turner, D. H. *Biochemistry* **1998**, *37*, 9379−9385. (e) Sugimoto, N.; Kierzek, R.; Turner, D. H. *Biochemistry* **1988**, *27*, 6384−6392. (f) Sugimoto, N.; Tomka, M.; Kierzek, R.; Bevilacqua, P. C.; Turner, D. H. *Nucleic Acids Res.* **1989**, *17*, 355−371. (g) Ohmichi, T.; Kool, E. T. *Nucleic Acids Res*. **2000**, *28*, 776−783.

(2) Mathews, D. H.; Burkard, M. E.; Freier, S. M.; Wyatt, J. R.; Turner, D. H. *RNA* **1999**, *5*, 1458−1469.

(3) Gluick, T. C.; Draper, D. E. *J. Mol. Biol*. **1994**, *241*, 246−262.

(4) (a) Freier, S. M.; Kierzek, R.; Jaeger, J. A.; Sugimoto, N.; Caruthers, M. H.; Neilson, T.; Turner, D. H. *Proc. Natl Acad. Sci. U.S.A.* **1986**, *83*, 9373−9377. (b) Turner, D. H.; Sugimoto, N.; Freier, S. M. *Annu. Rev. Biophys. Biophys. Chem.* **1988**, *17*, 167−192. (c) Xia, T.; SantaLucia, J., Jr.; Burkard, M. E.; Kierzek, R.; Schroeder, S. J.; Jiao, X.; Cox, C.; Turner, D. H. *Biochemistry* **1998**, *37*, 14719−14735. (d) Burkard, M. E.; Kierzek, R.; Turner, D. H. *J. Mol. Biol*. **1999**, *290*, 967−982. (e) Mathews, D. H.; Sabina, J.; Zuker, M.; Turner, D. H. *J. Mol. Biol*. **1999**, *288*, 911−940.

(5) (a) SantaLucia, J., Jr.; Allawi, H. T.; Seneviratne, P. A. *Biochemistry* **1996**, *35*, 3555−3562. (b) Allawi, H.T.; SantaLucia, J., Jr. *Biochemistry* **1997**, *36*, 10581−10594. (c) Allawi, H. T.; SantaLucia, J., Jr. *Nucleic Acids Res*. **1998**, *26*, 4925−4934. (d) Allawi, H. T.; SantaLucia, J., Jr. *Biochemistry* **1998**, *37*, 9435−9444. (e) Allawi, H. T.; SantaLucia, J., Jr. *Nucleic Acids Res*. **1998**, *26*, 2694−2701. (f) Allawi, H. T.; SantaLucia, J., Jr. *Biochemistry* **1998**, *37*, 2170−2179. (g) SantaLucia, J., Jr. *Proc. Natl. Acad. Sci. U.S.A.* **1998**, *95*, 1460−1465. (h) Peyret, N.; Seneviratne, P. A.; Allawi, H. T.; SantaLucia, J., Jr. *Biochemistry* **1999**, *38*, 3468−3477.

(6) Sugimoto, N.; Nakano, S.; Yoneyama, M.; Honda, K. *Nucleic Acids Res.* **1996**, *24*, 4501−4505.

(7) Doktycz, M. J.; Goldstein, R. F.; Paner, T. M.; Gallo, F. J.; Benight, A. S. *Biopolymers* **1992**, 32, 849−864.

(8) Sugimoto, N.; Nakano, S.; Katoh, M.; Matsumura, A.; Nakamuta, H.; Ohmichi, T.; Yoneyama, M.; Sasaki, M. *Biochemistry* **1995**, *34*, 11211−11216.

10.1021/ja001779f CCC: $19.00 © 2000 American Chemical Society
Published on Web 11/04/2000

From a kinetic standpoint, typical data exist for the kinetic properties of the Watson−Crick base pairs.[10−12] The forward rates, k_{on}, of the duplex formation of nucleic acids are about 10^5−10^7 $M^{-1}s^{-1}$, and depend on the sequence and salt conditions. The activation energy for k_{on} is negative or zero.[13] The dissociation rates significantly depend on the size, sequence, condition, and complementarity of the nucleic acids. Furthermore, the zip-up model has been assumed to be the mechanism of the Watson−Crick base pair formation.[10−12] In this model, the rate-limiting step is the formation of a nucleus containing 2−3 base pairs. The double helix then zips up after formation of the nucleus. Kinetic data for the non-Watson−Crick base pair also have been determined.[14] However, the kinetic effects of the non-Watson−Crick pairs on the helix formation are not easily understood due to the small number of data and unexpected results,[14] although the kinetic data are useful for understanding the contributions of the unpaired regions to the DNA and RNA foldings. Thus, systematic kinetic data for the non-Watson−Crick pairs are needed as well as the recent thermodynamic data.

Bulge structure in the DNA duplex is created by the misincorporation or deletion of some nucleotides in the double helix during replication, and causes a frame shift mutation.[15] Catalytic DNA also has bulge structures within the catalytic core.[16] Furthermore, the bulge structure is important for binding between the protein and DNA.[17] Thus, the bulge structure in DNA is one of the important non-Watson−Crick pairs. Here, we investigated the detailed kinetic behaviors of the DNA double strand with one bulged nucleotide using a temperature-jump method. Our data indicate that the activation energy for the helix association depends on both the bulged nucleotide and its flanking base pairs. Moreover, we found that the energy diagrams of the helix formation for the bulged helices can be estimated using the nearest-neighbor parameters for the DNA/DNA helix similar to a fully matched double helix.

Experimental Section

Materials. All of the oligodeoxyribonucleotides were chemically synthesized on a solid support by the phosphoramidite method using an Applied Biosystems model 391 DNA/RNA synthesizer. The synthesized DNA oligonucleotides were removed from the CPG (controlled pore glass) column by treatment with 25% concentrated ammonia at 55 °C for 8 h. After drying in a vacuum, the DNA oligonucleotides were passed through a Poly-Pak cartridge (Gren Research Co., Ltd.) with 2% TFA (trifluoroacetic acid) to remove the dimethoxytrityl groups. After the deblocking operations, the final purities of the DNA oligonucleotides were confirmed to be greater than at least 99% by HPLC (high performance liquid chromatography) on a TSKgel Oligo DNA RP column (4.6 mm i.d. × 15 cm, TOSOH) with a linear-gradient of 0−50% methanol/H_2O containing 0.1 M TEAA (triethylamine acetate) (pH 7.0). The obtained DNA oligonucleotides were desalted again with a C18 Sep-Pak cartridge. The oligonucleotide concentration was determined from the absorbance at 260 nm with single-strand extinction coefficients calculated from the mononucleotide and dinucleotide data of a nearest-neighbor approximation.[18]

UV Measurements. Absorbance measurements were made on Hitachi U-3200 and U-3210 spectrophotometers. Melting curves (absorbance versus temperature curves) were measured at 260 nm with a Hitachi SPR-10 thermoprogrammer. The temperature was monitored with the temperature transducer mounted in the spindle of the thermoelectric cuvette holder. The temperature readings from the transducer were calibrated by measuring the voltage produced by the thermocouple. The water condensation on the cuvette exterior in a low-temperature range was avoided by flushing with a constant stream of dry N_2 gas. All of the samples were initially heated to 90 °C, cooled to 0 °C for 3 °C/min, and stored at 0 °C for 10 min. The heating rate was 0.5 °C/min for the 0.1 cm path length cuvette and 1.0 °C/min for the 1.0 cm path length cuvette. The UV melting curves were collected in NaCl-phosphate buffer which contains 1 M NaCl, 10 mM Na_2HPO_4 and 1 mM Na_2EDTA (pH 7.0).

Determination of Thermodynamics for Duplex Formation. We evaluated the enthalpy ($\Delta H°$), entropy ($\Delta S°$), and free energy ($\Delta G°_{25}$) changes at 25 °C for the double helix formation from plots of T_m^{-1} versus $\log(C_t/4)$. These thermodynamic values were analyzed by the following equations:[18]

$$T_m^{-1} = 2.303R \log(C_t/4)/\Delta H° + \Delta S°/\Delta H° \quad (1)$$

$$G°_{25} = \Delta H° - 298.15\Delta S° \quad (2)$$

where C_t is the total strand concentration and R is the gas constant. To increase the accuracy of these determinations, the melting curves were fitted with a procedure to obtain the thermodynamic parameters as described elsewhere.[19] This method makes estimates of the thermodynamic values from the shape of each melting curve.

Circular Dichroism (CD) Measurements. The circular dichroism (CD) spectra of the samples were obtained with a 0.1 cm path length quartz cell at 5 °C using a JASCO J-600 spectrophotometer (JASCO Co., Ltd.) interfaced to a Dell OptiPlex GXi computer. The cell holder was thermostated by a JASCO PTC-348 temperature controller and the cuvette-holding chamber was flushed with a constant steam of dry N_2 gas to avoid water condensation on the cuvette exterior. All of the CD spectra were the averages of three scans made at 0.1 nm intervals from 320 to 200 nm. The concentration of the samples was 70 μM in 1 M NaCl/10 mM phosphate/1 mM Na_2EDTA (pH 7.0).

Temperature-jump Kinetics. The temperature-jump instrument was manufactured by Otsuka Electronics (Japan). The data collection and data analysis were controlled by an NEC PC9801 VX personal computer using the Otsuka Electronics measuring program. The light path length is 1.0 cm, and the sample volume is 1.2 mL. The light source was a D2 lamp and all relaxations were measured at 260 nm with a 14-nm band-pass. The range of the temperature jump was determined to be 3.2 °C for a capacitor charged at 12.5 kV in a solution containing 1 M NaCl by calibration of a test sample using the phenolphthalein-β-cyclodextrin inclusion reaction.[13] The reaction temperature was controlled by setting the initial sample temperature at 3.2 °C lower than the final sample temperature. The relaxation curves were measured 5−10 times for each experiment, and the relaxation times were evaluated for the averaged relaxation curves. Analysis of kinetic data is described in the Results section.

(9) (a) Schweitzer, B. A.; Kool, E. T. *J. Am. Chem. Soc*. **1995**, *117*, 7, 1863−1872. (b) Guckian, K. M.; Barbara, A.; Schweitzer, B. A.; Ren, R. X.-F.; Sheils, C. J.; Paris, P. L.; Tahmassebi, D. C.; Kool, E. T. *J. Am. Chem. Soc.* **1996**, *118*, 8182−8183. (c) Matray, T. J.; Kool, E. T. *J. Am. Chem. Soc.* **1998**, *120*, 6191−6192. (d) Guckian, K. M.; Schweitzer, B. A.; Ren, R. X.-F.; Sheils, C. J.; Tahmassebi, D. C.; Kool, E. T. *J. Am. Chem. Soc.* **2000**, *122*, 2213−2222.

(10) Craig, M. E.; Crothers, D. M.; Doty, P. *J. Mol. Biol.* **1971**, *62*, 383−401.

(11) (a) Pörschke, D.; Eigan, M. *J. Mol. Biol.* **1971**, *62*, 361−381. (b) Pörschke, D.; Uhlenbeck, O. C.; Martin, F. H. *Biopolymers* **1973**, *12*, 1313−1335.

(12) Williams, A. P.; Longfellow, C. E.; Freier, S. M.; Kierzek, R.; Turner, D. H *Biochemistry* **1989**, *28*, 4283−4291.

(13) Turner, D. H.; Sugimoto, N.; Freier S. M. In *Landolt-Bornstein Nucleic Acids*; Saenger, W. R., Ed.; Springer-Verlag: Berlin, Germany, 1990: Vol. 1c, Chapter 3.6.

(14) Chu, Y. G.; Tinoco, I., Jr. *Biopolymers* **1983**, *22*, 1235−1246.

(15) (a)Fishel, R.; Ewel, A.; Lee, S.; Lescoe, M. K.; Griffith, J. *Science* **1994**, *266*, 1403−1405. (b) Parsons, R.; Li, G. M.; Longley, M. J.; Fang, W. H.; Papadopoulos, N.; Jen, J.; de la Chapelle, A.; Kinzler, K. W.; Vogelstein, B.; Modrich, P. *Cell* **1993**, *75*, 1227−1237. (c) Umar, A.; Boyer, J. C.; Kunkel, T. A. *Science* **1994**, *266*, 814−816.

(16) Li, Y.; Liu, Y.; Breaker, R. R. *Biochemistry* **2000**, *39*, 3106−3114.

(17) Wang, Y. H.; Bortner, C. D.; Griffith, J. *J. Biol. Chem.* **1993**, *268*, 17571−17577.

(18) Richards, E. G. In *Handbook of Biochemistry and Molecular Biology: Nucleic Acids*, 3rd ed.; Fasman, G. D., Ed.; CRC Press: Cleveland, OH, 1975; Vol. 1, p 597.

(19) Nakano, S.; Fujimoto, M.; Hara, H.; Sugimoto, N. *Nucleic Acids Res*. **1999**, *27*, 2957−2965.

CORE : dTAGGTTATAA / dATCCAATATT

GCG-bulge : dTAG^{C}GTTATAA / dATC - CAATATT

GAG-bulge : dTAG^{A}GTTATAA / dATC - CAATATT

TCT-bulge : dTAGGT^{C}TATAA / dATCCA - ATATT

ACT-bulge : dTAGGTTA^{C}TAA / dATCCAAT - ATT

Figure 1. Sequences and predicted secondary structures of CORE and bulged helixes.

Results

Sequence Design. Earlier kinetic studies assumed a zip-up model as the mechanism for the short helix formation with Watson−Crick base pairs.[10−12] This model shows that only one helical region is allowed as the initiation site per duplex. This suggests that if the helix is a homooligonucleiotide, there are many initiation sites within the double helix. Many initiation sites make many reaction pathways for one helix formation so that the kinetic data would be complex. Furthermore, self-aggregation of the single-strand oligonucleotide leads to unexplained kinetic result.[14] For that reason, the core DNA/DNA helix, d(TAGGTTATAA)/d(ATCCAATATT), is carefully designed to be a heterooligonucleotide and unfavorable for intramolecular secondary structures (Figure 1). In fact, the predicted free energies ($\Delta G°_{37}$) of the intramolecular second structures for d(TAGGTTATAA) and d(ATCCAATATT) are +2.0 and +1.8 kcal/mol, respectively. The CD spectrum of d(TAGGTTATAA)/d(ATCCAATATT) indicated a normal B-form structure (data not shown). Thus, these data suggest that this core helix is a good control helix. To investigate the effects of the bulge nucleotide and its flanking base pairs, we also prepared four bulged helices (GCG-bulge helix, GAG-bulge helix, TCT-bulge helix, and ACT-bulge helix; Figure 1). All of the CD spectra of the bulged helices indicated normal B-form spectra similar to the CORE-helix. The insert of the bulged nucleotide sometimes leads to a new shoulder peak at 280 nm which is due to the single-stranded aggregation.[20] Thus, the insertion of one bulged nucleotide into the core helix does not alter the B-form conformation.

Thermodynamic Parameters. The thermodynamic parameters of each duplex were initially measured to investigate whether the duplex shows a two-state transition. Typical melting curves are shown in Figure 2. Since some lower baselines with bulged helices could not be observed, all of the melting temperatures (T_m) were calculated from the maximum point of the first derivative of the absorbance versus temperature profile, dA/dT. Figure 3 shows typical T_m^{-1} and log(C_t/4) plots of the CORE-helix, GCG-bulge helix, and ACT-bulge helix. In Figure 3, the melting temperatures decrease with decreasing total strand concentrations, and the T_m^{-1} and log(C_t/4) plots are linear. The plots gave us the thermodynamic parameters ($\Delta H°$, $\Delta S°$, and $\Delta G°_{25}$) for the duplex formation as shown in Table 1. For example, the order of $-\Delta G°_{25}$ was CORE-helix > GCG-bulge helix > GAG-bulge helix > TCT-bulge helix > ACT-bulge helix. Whether these duplexes exhibit a two-state transition can be determined by comparison of the curve-fitting procedure.[19,21] In this study, the differences between these thermodynamic parameters were within 10% (Table 1). Thus, the data suggest that there are not multiple transition processes for the single-strand self-transition, and the melting behavior of the duplexes can be regarded as a two-state transition. The final thermodynamic parameters are evaluated from the average values obtained from the curve fitting and T_m^{-1} versus log(C_t/4) plots.

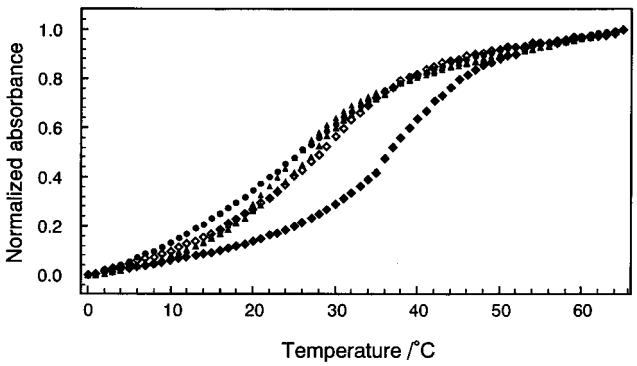

Figure 2. Normalized melting curves of core (closed diamonds), GCG bulge (open diamonds), GAG bulge (closed triangles), TCT bulge (open triangles), and ACT bulge (closed circles). All melting curves were measured at 100 mM total strand concentration in 1 M NaCl buffer (pH 7.0).

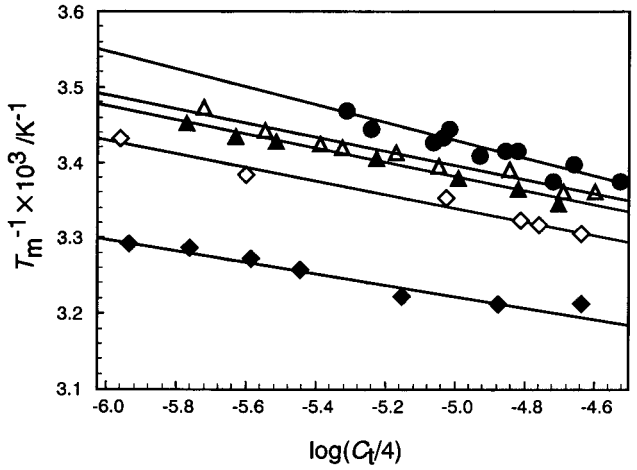

Figure 3. T_m^{-1} vs log(C_t/4) plots of core (closed diamonds), GCG bulge (open diamonds), GAG bulge (closed triangles), TCT bulge (open triangles), and ACT bulge (closed circles).

Kinetic Parameters. Figure 4 shows a typical temperature-jump relaxation curve and its curve fit obtained by one exponential fitting. Some relaxation curves had so fast component in the millisecond range before the main relaxation. This fast component is frequently observed in TCT-bulge and ACT-bulge helices. A similar component is reported and estimated to be due to fraying of the terminal nucleotides, single strand unstacking, or conformational transition.[10,11,22−24] However, as this minor component showed a very small amplitude, the error in the main relaxation time was within 5% when compared with that obtained by one exponential fitting. Thus, the main relaxation time was used in the calculation of the rate constant.

(20) Longfellow, C. E.; Kierzek, R.; Turner, D. H. *Biochemistry* **1990**, *29*, 278−285.

(21) Petersheim, M.; Turner, D. H. *Biochemistry* **1983**, *22*, 256−263.

(22) Tibanyenda, N.; De Bruin, S. H.; Haasnoot, C.; van der Marel, G. A.; van Boom, J. H.; Hilbers, C. W. *Eur. J. Biochem.* **1984**, *139*, 19−27.

(23) Hoggett, J. G.; Maass, G. *Ber. Bunsen-Ges. Phys. Chem.* **1971**,*75*, 45−54.

(24) Freier, S. M.; Albergo, D. D.; Turner, D. H. *Biopolymers* **1983**, *22*, 1107−1131.

Table 1. Thermodynamic Parameters for Helix Formation in 1 M NaCl-phosphate Buffer[a]

	T_m^{-1} vs log (C_t/4) parameter			curve fit parameter		
	$-\Delta H°$ kcal mol^{-1}	$-\Delta S°$ cal mol^{-1} K^{-1}	$-\Delta G°_{25}$ kcal mol^{-1}	$-\Delta H°$ kcal mol^{-1}	$-\Delta S°$ cal mol^{-1} K^{-1}	$-\Delta G°_{25}$ kcal mol^{-1}
dTAGGTTATAA dATCCAATATT	67.1 ± 1.1	194 ± 31	9.32 ± 1.2	65.5 ± 4.1	189 ± 13	9.29 ± 0.29
dTAG^{C}GTTATAA dATC − CAATATT	63.4 ± 3.8	187 ± 12	7.51 ± 0.47	61.3 ± 1.0	181 ± 3.3	7.40 ± 0.15
dTAG^{A}GTTATAA dATC − CAATATT	50.3 ± 6.8	146 ± 20	6.66 ± 0.80	47.5 ± 2.0	138 ± 7.0	6.39 ± 0.14
dTAGGT^{C}TATAA dATCCA − ATATT	49.4 ± 2.8	145 ± 8.4	6.17 ± 0.34	50.6 ± 1.8	150 ± 6.1	5.80 ± 0.73
dTAGGTTA^{C}TAA dATCCAAT − ATT	39.4 ± 4.7	112 ± 14	5.94 ± 0.52	36.4 ± 2.3	103 ± 7.8	5.85 ± 0.14

[a] The buffer contains 1 M NaCl, 10 mM Na_2HPO_4, and 1 mM Na_2EDTA (pH 7.0).

Table 2. Kinetic Parameters for Helix Formatin[a]

	$k_{+1} \times 10^{-7}$ (25 °C) M^{-1} s^{-1}	$-k_{-1}$ (25 °C) s^{-1}	E_{a+1} kcal mol^{-1}	E_{a-1} kcal mol^{-1}	$\Delta S^{‡}_{+1}$ cal mol^{-1} K^{-1}	$\Delta S^{‡}_{-1}$ cal mol^{-1} K^{-1}
dTAGGTTATAA dATCCAATATT	2.1	3.2	−3.4	61.9	−38.3	149
dTAG^{C}GTTATAA dATC − CAATATT	1.0	34.6	−13.5	50.9	−73.8	118
dTAG^{A}GTTATAA dATC − CAATATT	1.1	180	−1.6	48.7	−33.7	112
dTAGGT^{C}TATAA dATCCA − ATATT	1.4	560	0.2	49.6	−27.1	118
dTAGGTTA^{C}TAA dATCCAAT − ATT	0.3	142	4.3	43.6	−16.5	95.3

[a] Errors in k_{+1} and k_{-1} are estimated as ±10%.

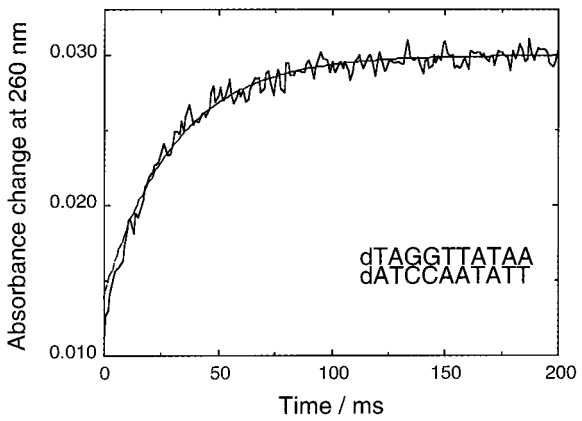

Figure 4. Temperature-jump kinetic trace of 10 μM dTAGGTTATAA·dATCCAATATT at 25 °C in 1 M NaCl buffer (pH 7.0).

The data were analyzed by a two-state model, because the melting experiment showed all the bulged helix formations to be two-state transitions. For a reaction in the following scheme:

$$A + B \underset{k_{-1}}{\overset{k_{+1}}{\rightleftharpoons}} AB \tag{3}$$

the association rate constant (k_{+1}) and the dissociation rate constant (k_{-1}) for the double helix formation were obtained using the following equation:[25]

$$1/\tau^2 = 2\,k_{+1}k_{-1}C_t + k_{-1}^2 \tag{4}$$

Here, τ is the relaxation time and C_t is the total strand concentration. Figure 5 shows the τ^{-2} vs C_t plots of the CORE-helix, GCG-bulge helix, and ACT-bulge helix. Within the experimental temperature range, the plots are linear. The intercepts of these plots are, however, very small and probably give large errors. Therefore, we employed only the slope and determined k_{-1} using the following equation:[12]

$$k_{+1} = (\text{slope}\cdot K_{eq}/2)^{1/2} \tag{5}$$

$$k_{-1} = k_{+1}/K_{eq} \tag{6}$$

where the equilibrium constant, K_{eq}, was obtained from our melting experiments. Figure 6 shows the Arrhenius plots for association and dissociation of the CORE-helix, GCG-bulge helix, and ACT-bulge helix. The activation energy, E_a, is derived from slope of the plot. The activation entropy, $\Delta S^{‡}$, is derived from the Eyring equation:

$$k = (eRT/Nh)\exp(-E_a/RT)\exp(\Delta S^{‡}/R) \tag{7}$$

where e is the base for the natural logarithms, N is Avogadro's number, and h is Planck's constant. Table 2 summarizes the extracted rate constants and the activation parameters. The insertion of one bulged nucleotide slightly decreased the association rate constant and greatly increased the dissociation rate constant, which was also seen in the DNAs with mismatched nucleotides.[20] The activation energies for the helix formation are from −13.5 to +4.3 kcal/mol. These results indicate that the activation energies are dependent on both the bulged nucleotide and its flanking base pairs as well as the thermodynamic parameters for the bulged helices.

Analysis for Kinetic Behavior Using Nearest-Neighbor Parameters. The zipper model is assumed to the mechanism

(25) Nelson, J. W.; Tinoco, I., Jr. *Biochemistry* **1982**, *21*, 5289−5295.

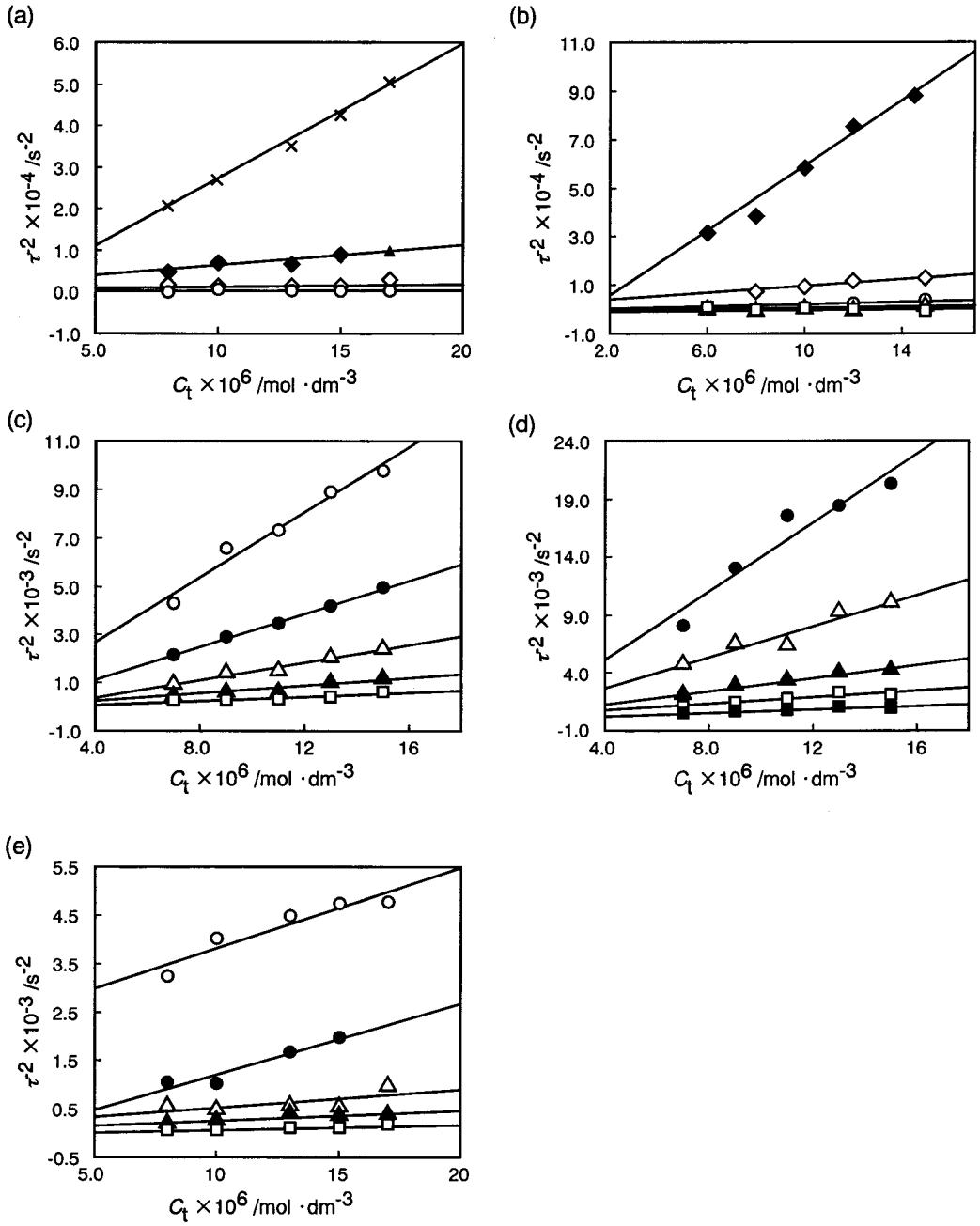

Figure 5. τ^{-2} vs C_t plots of (a) CORE, (b) GCG-bulge, (c) GAG-bulge, (d) TCT-bulge, and (e) ACT-bulge at 7.5 °C (closed squares), 10 °C (open squares), 12.5 °C (closed triangles), 15 °C (open triangles), 17.5 °C (closed circles), 20 °C (open circles), 25 °C (closed diamonds), 30 °C (open diamonds), and 35 °C (crosses) in 1 M NaCl buffer (pH7.0).

of the fully matched helix formation.[10−12] For the zipper model, the rate-determining step is the formation of a nucleus containing a small number of base pairs. The double helix can then zip up after the formation of the nucleus. Furthermore, it seems that the activation energies for k_1 provide the number of base pairs required for nucleation.[11,12] The activation energy, E_a, is given by $E_a = \Delta H°_{n-1} + E_{a,n-1\rightarrow n}$, where $E_{a,n-1\rightarrow n}$ is the activation energy for the elementary rate between the intermediates $n-1$ and n. Previous kinetic data suggest that $E_{a,n-1\rightarrow n}$ is roughly 5 kcal/mol which is mainly due to the single-stacking energy.[26,27] The $\Delta H°_{n-1}$ is the enthalpy change between single strands and the $n-1$ intermediate. Our data indicate that the enthalpy changes determined by the kinetic experiment are in agreement with the values determined by the thermodynamic measurements. For example, the enthalpy change for the CORE-helix that is given by $\Delta H° = E_{a+1} - E_{a-1}$ was found to be −65.4 kcal/mol. This value is similar to the value of −66.3 kcal/mol determined by the melting experiment. The nearest-neighbor model is useful in estimating the stability of the double helix.[4−8] The new nearest-neighbor parameters for the DNA/DNA helix have been reported by our group and that of SantaLucia[5,6] The predicted values of $\Delta H°$, $\Delta S°$, and $\Delta G°_{25}$ for the CORE-helix using our parameters are −67.7 kcal/mol, −193.5 cal/mol K, and −10.1 kcal/mol, respectively. The differences between the measured values and the predicted ones are 0.6, 1.3, and 7.0% for $\Delta H°$, $\Delta S°$, and $\Delta G°_{25}$, respectively. In the case of SantaLucia's parameters, the differences are 3.3, 4.1% and 0%, respectively. These results indicate that the measured values are in good agreement with the predicted ones. Thus, it seems

(26) Dewey, T. G.; Turner, D. H. *Biochemistry* **1979**, *18*, 5757−5762.
(27) Freier, S. M.; Hill, K. O.; Dewey, T. G.; Marky, L. A.; Breslauer, K. J.; Turner, D. H. *Biochemistry* **1981**, *20*, 1419−1426.

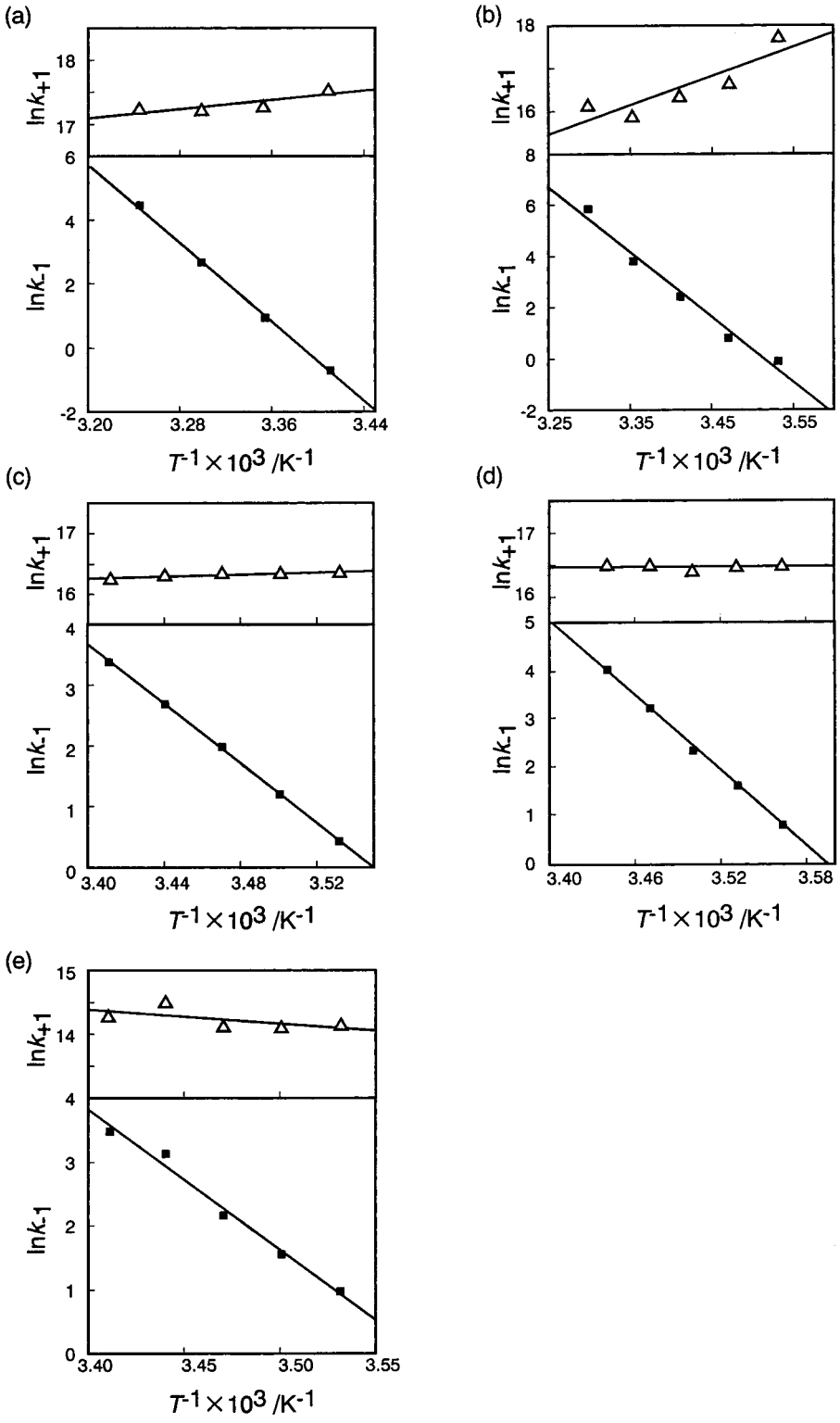

Figure 6. Arrhenius plots of (a) CORE, (b) GCG-bulge, (c) GAG-bulge, (d) TCT-bulge, and (e) ACT-bulge in 1 M NaCl NaCl buffer (pH7.0).

that the $\Delta H°_{n-1}$ value for each step can be estimated using the nearest-neighbor parameters for the DNA/DNA helix.

Figure 7A shows the energy diagram for the CORE-helix formation. The energy value for each step is calculated using our nearest-neighbor parameters. From a thermodynamic standpoint, it is considered that after making the initiation base pair, an energetically more favorable second base pair is formed. When a nucleus is one GC pair, the $\Delta H°_{n-1}$ value for one GC pair as the initiation is 0.6 kcal/mol, then the overall activation energy is $E_a = 0.6 + 5 = 5.6$ kcal/mol. This value is positive. When a nucleus is two GC pairs such as seen in Figure 7A, the $\Delta H°_{n-1}$ value for the two GC pairs is -10.3 kcal/mol and the overall activation energy becomes $E_a = -10.3 + 5 = -5.3$ kcal/mol. This estimated value is in fair agreement with the measured value of -3.4 kcal/mol. When a nucleus is three base pairs, GGT/ACC, the estimated activation energy of -14.7 kcal/mol is much smaller than that of the measurement. Thus, it seems that the nucleus of the CORE-helix is the formation of

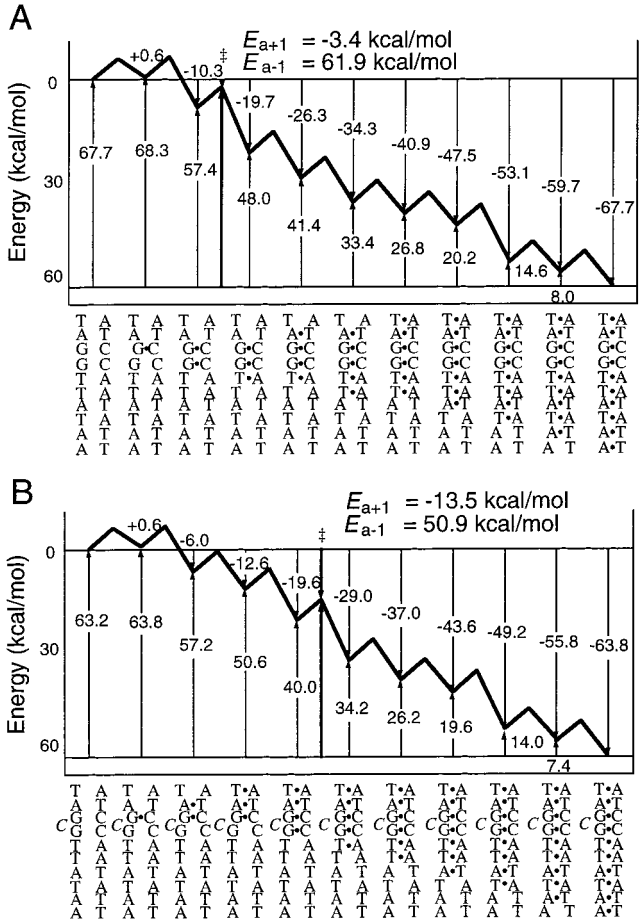

Figure 7. Schematic energy diagrams for association and dissociation reactions with (A) CORE helix and (B) GCG-bulge helix.

two GC pairs. This result is also supported by SantaLucia's parameters with an overall activation energy of $E_a = -7.9 + 5 = -2.9$ kcal/mol. This estimated value is also in good agreement with the measured value. The number of nucleus base pairs analyzed by the nearest-neighbor parameters is the same as the previous typical data.[13] Thus, these results suggest that the activation energies can be understood by an analysis of the enthalpy based on the nearest-neighbor parameters.

The bulge effect on the thermodynamic property can be estimated using the nearest-neighbor model as well as the effect of the Watson−Crick pairs.[20] The enthalpy change contributed by the insertion of one bulge is calculated by taking the difference in stabilities between the duplexes with and without the bulge and adding back the stacking stability of base pairs broken by the bulge. For example, the enthalpy change for the CGC-bulge is calculated by the following equation:

$$\Delta H^\circ_{(\text{bulge})} = \Delta H^\circ_{(\text{CGC-bulge})} - \Delta H^\circ_{(\text{CORE-helix})} + \Delta H^\circ_{(\text{GG/CC})} \quad (8)$$

where $\Delta H^\circ_{(\text{CGC-bulge})}$ and $\Delta H^\circ_{(\text{CORE-helix})}$ are the enthalpy changes of the duplex formations determined by optical melting and $\Delta H^\circ_{(\text{GG/CC})}$ is an enthalpy change predicted by the nearest neighbor parameters. The $\Delta H^\circ_{(\text{bulge})}$ is an enthalpy change increment of the bulged helix. The calculated bulge parameters are shown in Table 3. These values were estimated by using our nearest-neighbor parameters because of the smaller error in the enthalpy change for the CORE-helix between the predicted and the observed ones. Attempts were then made to understand the bulged helix formation using these parameters.

Table 3. Thermodynamic Increments for Bulged Nucleotides

bulge sequence	ΔH° kcal mol^{-1}	ΔS° cal mol^{-1} K^{-1}	ΔG°_{25} kcal mol^{-1}
GCG C−C	−7.0	−20.9	−0.72
GAG C−C	+6.5	−21.1	+0.24
TCT A−A	+8.3	+22.1	+1.71
ACT T−A	+22.8	+68.8	+2.29

The overall activation energy for the GCG-bulge is −13.3 kcal/mol. This value is smaller than those for the nucleus containing the 2−3 base pairs. For example, when a nucleus is 3 base pairs, TAG/CTA, the estimated activation energy is −7.6 (= −12.6 + 5) kcal/mol. Figure 7B shows the energy diagram for the helix formation of the GCG-bulge helix. The thermodynamic parameters in Table 3 were used as the nearest-neighbor parameters of the bulged nucleotide. When the nucleus of the GCG-helix is the formation of 4 base pairs containing one bulge, TAGCG/CCTA (C is bulged nucleotide), the E_a value of −13.5 kcal/mol is similar to the predicted value of −14.6 (= −19.6 + 5) kcal/mol (Figure 7B). Furthermore, the E_{a-1} value of 50.9 kcal/mol is also in agreement with the estimated one of 45.0 kcal/mol. In the case of the GAG-bulge helix, the observed E_a value is −1.6 kcal/mol which is similar to the one for the CORE-helix. The E_{a-1} value of 48.7 kcal/mol for the GAG-bulge is, however, smaller than that of 61.9 kcal/mol for the CORE-helix. The rate-limiting step in the dissociation of a short helix is the breaking of most of the base pairs, presumably to generate the fast-equilibrating nucleation structure seen in the strand combination.[28] Thus, the rate-limiting step during the association of the GAG-helix is not likely the formation of two base pairs such as that for the CORE-helix. The E_{a-1} value of 48.7 kcal/mol for the GAG-bulge is almost the same as 50.9 kcal/mol for the GCG-helix. The overall activation energy of −1.6 kcal/mol is very similar to the estimated values of − 1.1 kcal/mol for the formation of 4 base pairs containing one bulge, TAGAG/CCTA. Thus, the nucleus during the association of the GAG-helix is likely the formation of the bulge structure similar to that of the GCG-bulge helix. The E_a values of 0.2 and 4.3 kcal/mol for the TCT-bulge helix and ACT-bulge helix are also close to the estimated values of −2.1 kcal/mol for GTCTA/TAAC and 3.8 kcal/mol for GTTACT/ATAAC, respectively. These bulged nucleotide positions are different from the GCG-bulge and GAG-bulge. A previous study, however, indicates that mismatches more than three base pairs from the end are independent of the positions and are well predicted with the nearest-neighbor parameters.[5h] The estimations for the CTC-bulge and the ATC-bulge with the nearest-neighbor parameters would be reasonable. Thus, these data indicate that the nucleus and reaction mechanism with a bulged helix can be estimated using the nearest-neighbor parameters as well as the fully matched double helix.

Discussion

Factors Affecting Thermodynamic and Kinetic Properties with Bulged Helix. Our results demonstrate that the thermodynamic property for the bulged helix is useful for understanding the reaction pathway for bulged helix formation. These results also indicate that the kinetic properties with the bulged helix

(28) Canter, C. R.; Schimmel, P. R. *Biophysical Chemistry Part III: The behavior of Biological Macromolecules*; W. H. Freeman: San Francisco, 1980; Vol. 3, pp 1183−1264.

depend on the bulged nucleotides and flanking base pairs as well as the thermodynamic properties. Previous thermodynamic and structural studies allow us to understand the different forces that contribute to the sequence dependence on both the thermodynamic and kinetic properties of the bulged helix. Our thermodynamic data show that the free energy ($\Delta G^\circ_{25(\text{bulge})}$) of -0.72 kcal/mol for GCG-bulge is most favorable in the bulged helices. This value is 0.96 kcal/mol more stable than the value for the GAG-bulge that has the same flanking base pairs but a different bulged nucleotide. Previous thermodynamic studies show that pyrimidine bulges are more stable than purine bulges.[29] Our result is in agreement with the previous study. This difference can also be understood by structural studies.[30,31] Previous NMR studies show that the bulged A in GG or CC is stacked into the helix and the bulged C in GG is likely to be looped out. On the basis of these studies, it seems that the two flanking GC pairs retain hydrogen bonding and the stacking interaction by looping out the C bulge. This hypothesis is also supported by the most favorable ΔH° values with GCG-bulge in the bulged helices, because ΔH° contributes to hydrogen bonding and the stacking interaction.[32] On the other hand, the stacked conformation in the A bulge is likely to break the stacking interaction between two flanking base pairs. Thus, the difference between the GCG-bulge and GAG-bulge regions would be due to the location of the bulged nucleotides.

Our results also indicate the effect of the flanking base pairs on the bulged nucleotide. The free energy ($\Delta G^\circ_{25(\text{bulge})}$) for the GCG-bulge helix is 2.43 and 3.01 kcal/mol more stable than the TCT-bulge and ACT-bulge helices, respectively. The effect of the flanking base pair on the bulged ribonucleotide had been earlier investigated.[20] The flanking CG base pair in the RNA/RNA helix is more stable than the AU base pair. Thus, it is reasonable that the TCT and ACT bulge regions are less stable than that of the GCG-bulge. Although the unpaired region was a single mismatch, the effect of the flanking base pairs on the single mismatch was investigated.[5h] The data shows that the stability trend for the flanking base pairs on the 5′ side of the mismatch is G·C > C·G > A·T > T·A. Our data's trend is not in agreement with it because the TCT/AA is more stable than the ACT/AT (Table 3). Thus, the effect of the flanking base pairs on the single mismatch might be different from that on the bulged nucleotide.

Our data show that the entropy changes (ΔS°) during the bulged helix formations are more favorable than that in the CORE-helix. The differences among the bulged helices are approximately from 0 to 90 cal/mol K. The entropy change in the helix formation is due to the conformational entropy and the translational entropy.[31] One considers that the conformational entropies are identical for the bulged and nonbulged helices, because conformational entropy is due to the torsion angles with nucleotides. On the other hand, the translational entropy contains binding and release of water molecules and ions. Previous measurements of ΔS° and ΔV° for the bulged helix formation indicate that the water interaction is important for the bulged helix.[33] The finite-difference Poisson−Boltzmann (FDPB) approach also supports the contribution of hydration. It is reported that the binding and release of ions to a base contribute to the stability of a helix.[34] Thus the difference in ΔS° is likely to contribute to the binding and release of water molecules and ions. In the case of $\Delta S^\ddagger_{+1}$, the values for the GAG-bulge, TCT-bulge, and ACT-bulge are larger than that for the CORE-helix. The value of $\Delta S^\ddagger_{+1}$ for the GCG-bulge is smaller. If the difference in $\Delta S^\ddagger$ is likely to contribute to the translational entropy in the transition state as well as ΔS°, the differences in the activation energies for the bulged nucleotides and flanking base pairs would be due to the binding and release of water molecules and ions.

Predicting the Kinetics of the Bulged Helix. The kinetics of the bulged helix is predicted using the nearest-neighbor parameters. That is, the kinetic behavior of the helix formation can be based on the nearest-neighbor model as well as the thermodynamic properties. The equilibrium constants for the double helix formation can be predicted using the nearest-neighbor parameters because $K = \exp(-\Delta G^\circ/RT)$ and $\Delta G^\circ = \Delta H^\circ - T\Delta S^\circ$. The forward rates, k_{on}, are about 10^5-10^7 M^{-1} s^{-1}.[13] Thus, the value of k_{off} can be predicted because $K = k_{\text{on}}/k_{\text{off}}$. Our data for the bulged helices indicate that although the bulged nucleotides and the flanking base pairs are different, the formation of the bulged helix can be based on the zipper model. The kinetics of the double helix is predicted using the nearest-neighbor parameters as well as the fully matched double helix. When the value of 10^7 M^{-1} s^{-1} is used as k_{on}, the predicted k_{off} values for the GCG-bulge, GAG-bulge, and TCT-bulge are 34.6, 163, and 400 M^{-1} s^{-1}, respectively. These values are in good agreement with the experimental ones.

Furthermore, the forward rate constant in the zipper up model is given by the following equation:[12]

$$k_{+1} = K_{(0\sim n-1)}\, k_{(n-1,n)} \tag{9}$$

where $K_{(0\sim n-1)}$ is an equilibrium constant for the nucleus of the association reaction prior to the nucleus formation, and $k_{(n-1,n)}$ is an elementary rate constant for the formation of the nucleus containing n base pairs. Figure 7 shows that although the nucleus for the CORE-helix is different from that for GCG-bulge helix, the $k_{(n-1,n)}$ for the CORE-helix or GCG-bulge helix is the formation step for the AT base pair after the adjacent GC base pairing. The calculated $k_{(n-1,n)}$ value for CORE-helix is 4.0×10^7 s^{-1}. The value for GCG-bulge helix is 1.0×10^7 s^{-1}. These calculated forward rate constants ($k_{(n-1,n)}$) are within an order of magnitude. Thus, these data might indicate that the kinetic behavior of the helix formation can be based on nearest-neighbor model as well as the thermodynamic properties.

Recent structural studies indicate that bulge is a key structure in the folding of the catalytic nucleic acids (not DNAs).[35,36] In the case of P4−P6 domain of the group I ribozyme, two A-rich bulge regions form a long-distance base pair in the tertiary structure. An A-bulge is also a Mg^{2+} binding site. The kinetic pathways for the tertiary folding or metal binding are not yet clear and are of current intense interest. Although the number and position of our nearest-neighbor variation might not be enough to generalize the relationship between the activation

(29) Zieba, K.; Chu, T. M.; Kupke, D. W.; Marky, L. A. *Biochemistry* **1991**, *30*, 8018−8026.

(30) (a) Kalnik, M. W.; Norman, D. G.; Zagorski, M. G.; Swann, P. F.; Patel, D. J. *Biochemistry* **1989**, *28*, 294−303. (b) Kalnik, M. W.; Norman, D. G.; Swann, P. F.; Patel, D. J. *J. Biol. Chem.* **1990**, *256*, 636−647.

(31) Kalnik, M. W.; Norman, D. G.; Swann, P. F.; Patel, D. J. *J. Biol. Chem.* **1989**, *264*, 3702−3712.

(32) Burkard, M. E.; Turner, D. H.; Tinoco, I., Jr. In *RNA World*, 2nd ed.; Gesteland, R. F., Cech, T. R., Atkins, J. F., Eds.; Cold Spring Harbor Laboratory Press: Cold Spring Harbor, NY, 1999; pp 233−264.

(33) Zieba, K.; Chu, T. M.; Kupke, D. W.; Marky, L. A. *Biochemistry* **1991**, *30*, 8018−8026.

(34) Zacharias, M.; Sklenar, H. *Biophys J.* **1997**, 2990−3003.

(35) Cate, J. H.; Gooding, A. R.; Podell, E. Zhou, K.; Golden, B. L.; Kundrot, C. E.; Cech, T. R.; Doudna, J. A. *Science* **1996**, *273*, 1678−1685.

(36) Cate, J. H.; Hanna, R. L.; Doudna, J. A. *Nat. Struct. Biol.* **1997**, *4*, 553−558.

energy for the helix formation and the nearest-neighbor parameters for the bulged helices, our results demonstrate that the thermodynamic property for the non-Watson−Crick region is useful for understanding the mechanisms of formation for the unpaired helices. Thus, if more detailed effects of the sequence and metal binding on the thermodynamic properties for helix formations are investigated, the folding pathways for the catalytic nucleic acids (ribozymes and dexyribozymes) could be more exactly predicted.

Acknowledgment. We thank Professor Fu-Ming Chen, Tennessee State University, for a critical reading of the manuscript and helpful comments. This work was supported in part by Grants-in-Aid from the Ministry of Education, Science, Sports and Culture, Japan, and a Grant from "Research for the Future" Program of the Japan Society for the Promotion of Science.

JA001779F